JOURNAL OF MATERIALS SCIENCE **33** (1998) 4977–4985

Superplasticity of fine-grained Fe–C alloys prepared by ingot-and powder-processing routes

W. J. KIM
Hong-Ik University, Dept. Metallurgy and Material Science & Eng., Seoul, Korea 121-791

E. M. TALEFF
University of Texas at Austin, Dept. Aerospace & Engineering Mechanics, Austin, Texas 78712-1085

O. D. SHERBY
Stanford University, Dept. Materials Science & Eng., Stanford, CA 94305

Tensile elongation behavior of fine-grained Fe–C alloys has been investigated as a function of cementite volume fraction, degree of microstructural refinement, and the Zener-Hollomon parameter. The strain rate–stress relationships and creep strengths of Fe–C alloys with carbon contents from 1.3 to 5.25 wt. % C are found to be similar when grain size is similar. Superplastic ductility of ingot-processed alloys initially increases with carbon content but starts to decrease after 2.1% C. The increase of tensile ductility with carbon content below 2.1% C is attributed to a reduction in the case of dynamic grain growth associated with an increase in the number of fine cementite particles, whereas the decrease of tensile ductility above 2.1% C is due to an increase in the number of coarse cementite particles and an increase in the area of cementite/cementite grain boundaries. Superplastic ductility of Fe–C alloys with carbon contents higher than 2.1% C can be significantly enhanced when powder-processing routes are utilized instead of ingot-processing routes. Tensile elongation behavior of cementite-based alloys is revealed to be different from that of iron-based alloys when compared as a function of the Zener-Hollomon parameter.

1. Introduction

Superplasticity is the ability of a material to deform to very large tensile elongation at elevated temperatures, usually over several hundred percent elongation prior to failure. Superplasticity of ultra-high carbon steels (UHCs) with carbon concentrations varying from 0.8 to 3 pct C has been extensively studied by Sherby and his colleagues [1–9]. It was demonstrated that tensile elongations over 1000% could be obtained at the optimum combinations of temperature and strain rate. Recently, Kim and Sherby [10–12] examined the superplasticity of an extremely high-carbon alloy with a carbon content of 5.25% and found that its high-temperature mechanical behavior is different from that of superplastic metallic alloys but similar to that of superplastic ceramics. This is particularly true when tensile ductility behaviors are compared as a function of flow stress or Zener-Hollomon parameter.

Ingot-processing and powder-processing routes have been developed for the attainment of fine-grain, superplastic microstructures, in UHCs. In most cases ingot-processing routes were utilized for UHCs with carbon contents less than 2.1 percent, whereas powder-processing routes were adopted for the UHCs with carbon contents greater than 2.1 percent. It is the purpose of the present paper to investigate the overall tensile ductility behavior of Fe–C alloys, which have been prepared by both ingot- and powder-processing methods, as functions of microstructure, volume fraction of cementite.

2. Analysis and discussion

2.1. Mechanical behavior of Fe–C alloys

Hardness, test results, after water quenching from several temperatures, are shown in Fig. 1 for several Fe–C alloys. The A_1-transformation temperature is readily identified from the figure as $\sim 730\,^{\circ}C$ for all the alloys. The highest carbon-content material, 5.25% C (80 vol. % of cementite and 20 vol. % of ferrite) exhibits a very great hardness of about $R_c \sim 60$, in contrast to only $R_c \sim 20$ for the lowest carbon-content material, 1.25% C (20 vol. % of cementite and 80 vol. % of ferrite), when heated and quenched from just below the A_1 temperature. The plot in Fig. 1 clearly shows that hardness increases as volume fraction of cementite (or carbon content) increases. This result indicates that the strength of the cementite phase is much higher than that of the ferrite phase at low temperatures. The increase in hardness upon quenching from just above the A_1 temperature depends on the amount of austenite transformed into martensite. For example, only a slight

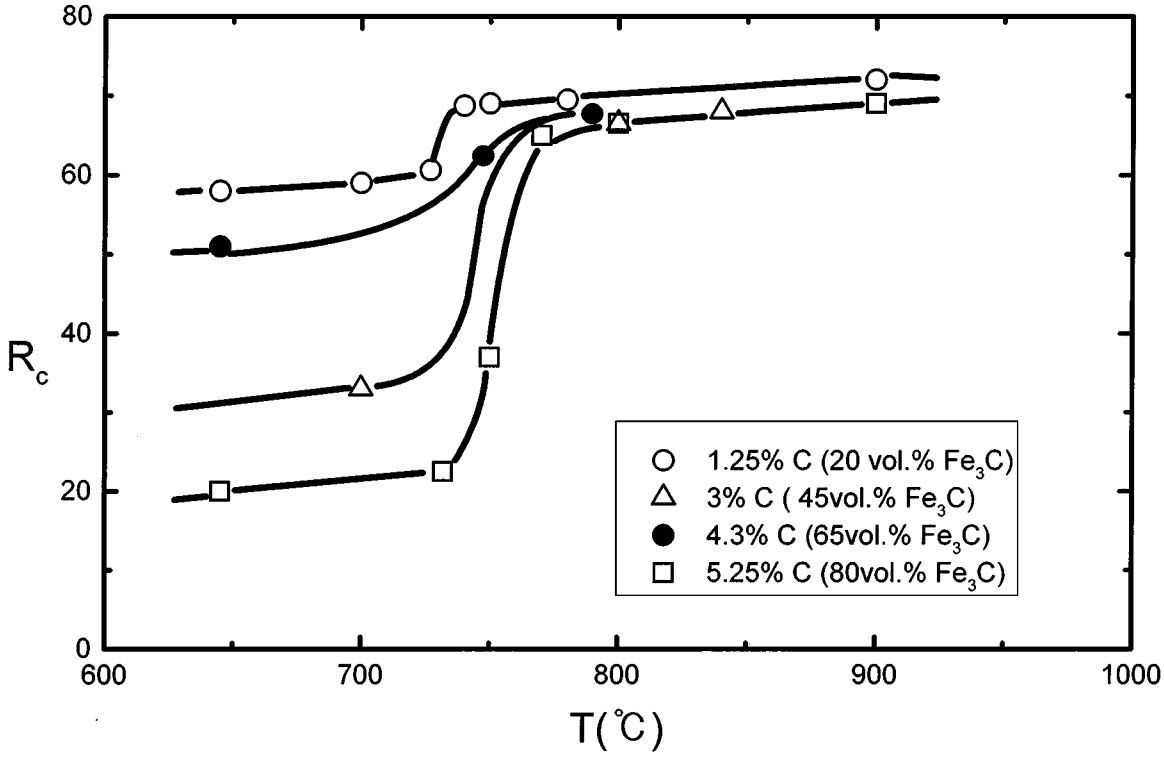

Figure 1 Hardness test results for Fe–C alloys.

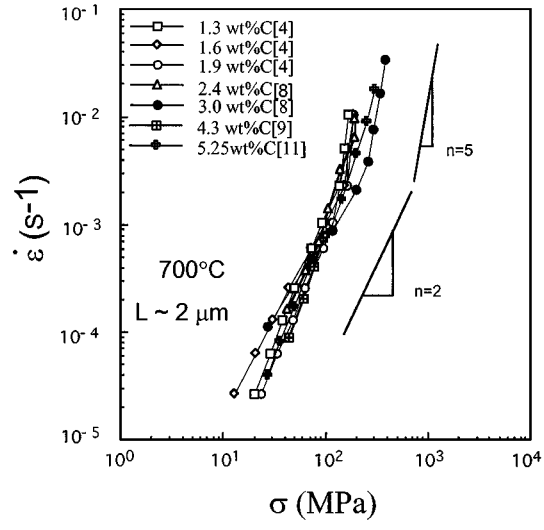

Figure 2 Strain rate-flow stress relationship for Fe–C alloys with a common linear intercept grain size of $\sim 2\,\mu$m.

increase in hardness is noted for the 5.25% alloy that has a small amount of iron-based phase, while a large increase in hardness is noted for 1.25% alloy where iron-based phase is the majority phase.

Strain-rate-change testing is typically used to determine the strain rate–stress relationship of an alloy deforming at elevated temperature. Fig. 2 shows data from such tests as logarithmic stress and logarithmic strain rate for the Fe–C alloys at a temperature of 700 °C. It should be noted that all the alloys in the plot have a similar linear-intercept grain size of 2 μm. The flow stress vs. strain rate relationship at elevated temperatures is typically expressed in the following constitutive equation,

$$\dot{\varepsilon} = A\left(\frac{b}{L}\right)^{p}(\sigma/E)^{n}\exp\left(\frac{-Q_c}{RT}\right) \qquad (1)$$

where $\dot{\varepsilon}$ is the steady-state creep rate, n is the stress exponent, L is the linear intercept grain size, p is the grain size component, b is the Burgers vector, σ is the flow stress, Q_c is the activation energy for creep, T is the absolute temperature, R is the gas constant, E is the dynamic Young's modulus and A is a material constant. The slope of the curves in Fig. 2, i.e. $d\log\sigma/d\log\dot{\varepsilon}$ represents the stress exponent, measured to be dependent upon the strain rate. The strain-rate-sensitivity exponent, m, is defined as $1/n$. All the Fe–C alloys in the present comparison have several aspects in common. First, all exhibit similar values of strain-rate-sensitivity, with low m values at high strain-rates and high m values at low strain-rates. In the high strain-rate regime, where m values as low as 0.2 are observed, slip (dislocation climb creep) is believed to control plastic deformation, and thus limited tensile ductility is expected. In the low strain-rate regime, however, grain boundary sliding, $m = 0.5$, is believed to be the rate-controlling deformation mechanism, and superplastic behavior is expected. Second, all the data of the Fe–C alloys superimpose onto a common curve, indicating that the creep strengths of the alloys are nearly identical. This result is in contrast to that shown in Fig. 1, where the alloy with the highest volume fraction of iron carbide was shown to be much stronger than that with the lowest fraction of iron carbide.

There are three types of grain boundaries present in the microstructures of the Fe–C alloys, which have two different phases (i.e., ferrite and cementite): ferrite/ferrite, cementite/ferrite, and cementite/cementite. The

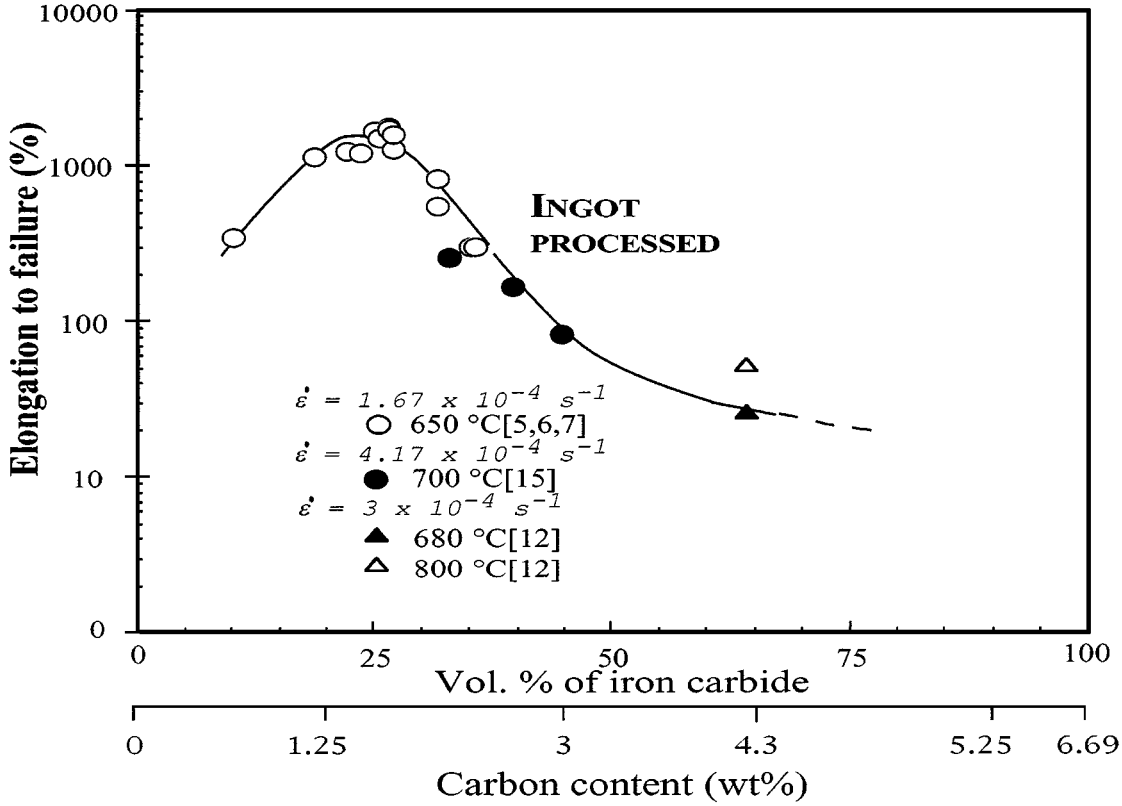

Figure 3 Tensile elongation of ingot-processed Fe–C alloys as a function of volume fraction of cementite.

amount (area) of each boundary type depends on the volume fraction of cementite. If the average size of ferrite is similar to that of cementite, the ferrite/cementite-type grain boundaries will be most abundant for the 3% C alloy composed of 50 vol. % ferrite and 50 vol. % cementite, whereas ferrite/ferrite type boundaries will be more common for the alloys with carbon contents of less than 3% C. Cementite/cementite-type grain boundaries will be more common for the alloys with carbon content higher than 3% C. The similar creep strengths observed at low strain rates can be interpreted to represent that grain-boundary-sliding mobility along ferrite/cementite boundaries is similar to that along ferrite/ferrite boundaries as well as that along cementite/cementite. The similarity of creep strength at high strain rates, where plastic deformation is controlled by slip, indicates that the strength of cementite itself is similar to that of ferrite at elevated temperature. Note that the strength difference between the two phases is quite large at low temperature.

2.2. Tensile ductility behavior as a function of volume fraction of cementite

A series of thermomechanical-processing routes have been developed [1–4] to refine the as-cast microstructure of Fe–C alloys into fine-grains suitable for superplasticity. For this purpose, ingot-processing routes were utilized for the alloys with carbon contents of less than 2.1% C, whereas powder-processing routes were utilized for the alloys with carbon contents higher than 2.1% C. Tensile elongation behavior of the ingot-processed alloys will be discussed first.

2.2.1. Ingot-processing routes

Fig. 3 shows a plot of tensile elongation data from ingot-processed Fe–C alloys as a function of volume fraction of cementite (or carbon content) at a given temperature (650 °C) and strain rate (1.64×10^{-4} s^{-1}). Some data obtained under different testing conditions are also plotted. As can be seen from the plot, tensile ductility of the ingot-processed Fe–C alloys is increased as carbon content increases from 0.8 to about 1.6% C and has its optimum value of elongation between 1.6 and 1.8% C. Tensile elongation, however, starts to decrease with an increase in carbon content beyond 1.8% C. The increase of tensile ductility with carbon content, observed between 0.8 and 1.8% C, can be attributed to an increase in the volume fraction of cementite. The increase of fine cementite particles per unit volume provides more pinning points for grain boundaries. This effect, in turn, reduces the grain growth rate, and thus the initial fine-grained microstructure can be maintained throughout testing. Fig. 4 is an SEM micrograph of the 1.8% C alloys where fine cementite particles are uniformly distributed in a ferrite matrix. The decrease of tensile ductility above 2.1% C, on the other hand, can be explained by the difficulty in obtaining an adequate solid-solution treatment beyond this composition. Solid-solution treatment that was developed to eliminate coarse cementite particles in the ferrite matrix cannot be utilized in the alloys with carbon content higher than 2.1% C because a fully-austenized structure cannot be obtained at any temperature. As a consequence, undissolved coarse cementite particles remain even after the solid-solution treatment. These carbides are extremely difficult to refine by subsequent

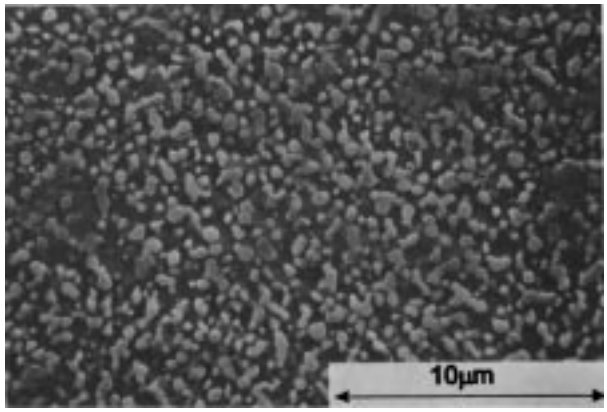

Figure 4 An SEM micrograph of the ingot-processed 1.8% C alloy.

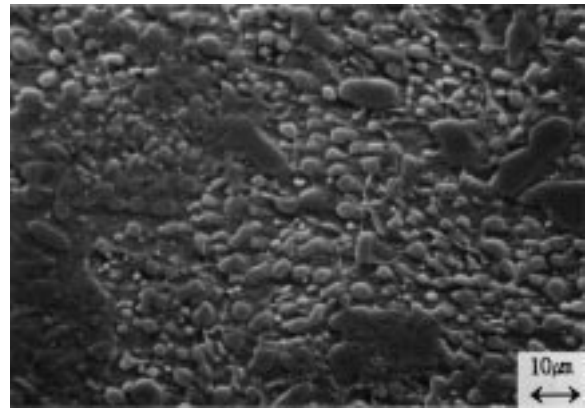

Figure 6 An SEM micrograph of the forged-only 3.0% C alloy.

thermo-mechanical treatments and tend to reduce tensile ductility by providing sites for cavity formation.

It was shown by Kim et al. [12–14] that the as-cast microstructures of the 3, 4.3 and 5.25% C alloys could not be significantly refined with conventional thermomechanical-processing routes originally developed for 0.8∼2.1% C alloys. Kim et al. utilized a special "stacking method" to refine the as-received microstructure of 3% C alloy [14]. The as-received ingot of 3% C alloy was hot-forged, hot-rolled, cut to several pieces and then stacked to be hot-pressed. The sequence of rolling, cutting, stacking and pressing was repeated several times to maximize the amount of plastic deformation. Fig. 5 is an SEM micrograph of the ingot-processed 3% C alloy, Fine cementite particles are present in the ferrite matrix. There still, however, exist non-fully-broken coarse proeutoid cementites with the size of about 10 μm even after such large plastic deformation. Recently, Kim and Sherby used hot forging-only until the rod of 3% C with a dia of 3 cm was obtained [14]. A very promising microstructure was resulted which is similar to that of the powder-processed 3% C material. Fig. 6 is the SEM micrograph of the forged-only 3% C material. The microstructure consists of fine-ferrite grains with fine cementites dispersed uniformly on matrix. Coarse cementites particles can be hardly detected anywhere. The strain rate–stress relationship, however, shows that the strain-rate-sensitivity exponent is as low as seven, and non-superplasticity is expected. This result is indicative of a possibility that the forged material consists of low-angle rather than high-angle boundaries. Kim et al. [13] utilized a special 'canning method' for the 5.25% C alloys, which has cementite as matrix, to minimize heat loss and thus prevent edge and surface cracking during rolling. This occurs because of fracture along the brittle cementite/cementite boundaries during pressing or rolling steps. It was demonstrated that a coarse cementite matrix could be refined by a considerably large amount of plastic deformation. Fig. 7 shows a schematic illustration of the major thermo-mechanical processing steps involved in microstructural refinement of the as-cast 5.25% alloy with corresponding SEM micrographs. A tensile elongation of 75% was achieved from the 5.25% alloy with the microstructure of Fig. 7b at 1035 °C. For the 4.3% alloys, Kim et al. [12] utilized an 'extrusion method' for microstructural refinement. The as-cast material was extruded at 1050 °C. A reasonably equiaxed and fine microstructure was obtained after an area reduction of 8.5 to 1. Fig. 8 is an SEM micrograph of the ingot-processed 4.3% C alloy. Fig. 9 is the strain rate–stress relationship in compression for the ingot-processed 3% C [14], 4.3% C [12] and 5.25% C alloys [13]. As can be seen, all the ingot-processed alloys exhibit *m* values lower than those of the powder-processed alloys shown in Fig. 2. Based on the above analyses, it can be concluded that the decrease in tensile ductility observed in the ingot-processed alloys with carbon contents beyond 2.1% C is principally attributed to the following three factors: the presence of coarse iron-carbide particles, the increase of cementite/cementite grain boundaries with carbon content and the decrease of *m* values lower than 0.5.

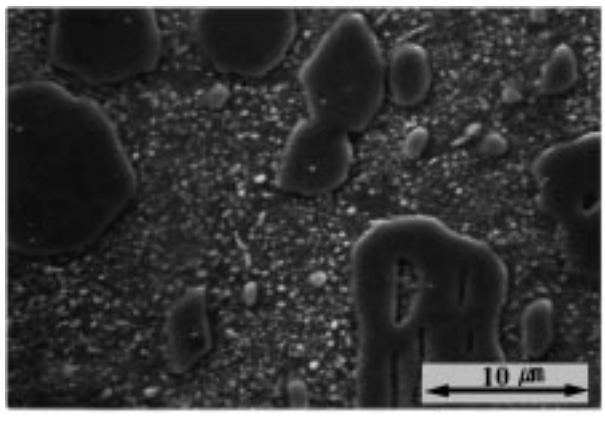

Figure 5 An SEM micrograph of the ingot-processed 3.0% C alloy.

2.2.2. Powder-processing routes

Coarse cementite particles can be eliminated during the initial stage of material preparation if powder-metallurgy methods are chosen instead of ingot-metallurgy ones. Figs 10 and 11 are SEM micrographs of the microstructures of powder-processed 3% C and 5.25% C alloys respectively. Both microstructures are uniformly fine and have equiaxed grains. In Fig. 12, tensile-elongation data of the powder-processed Fe–C alloys (beyond 2.1% C) are plotted as a function of cementite volume fraction (or carbon content) at

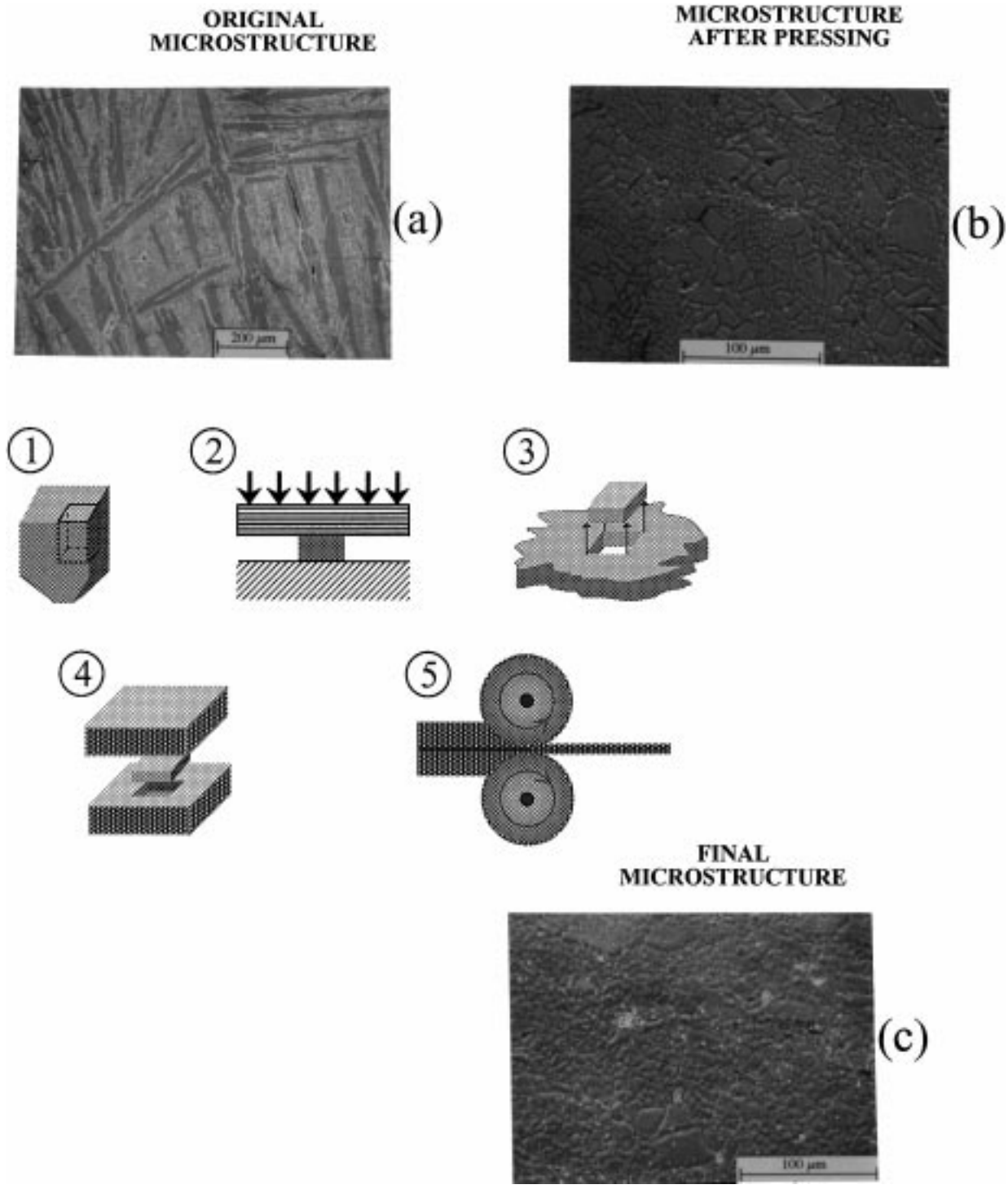

Figure 7 Schematic illustration of the major thermo-mechanical routes involved in microstructural refinement of the as-cast 5.25% C.

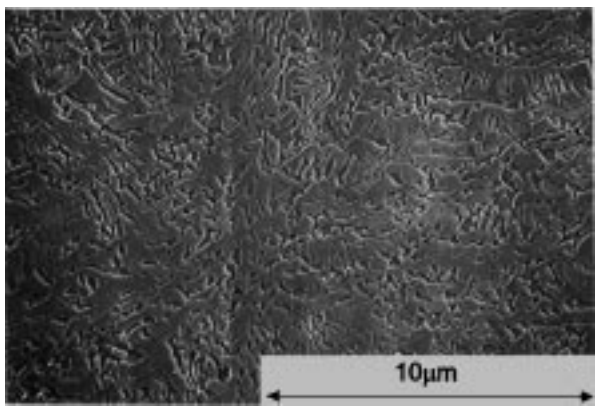

Figure 8 An SEM micrograph of the ingot-processed 4.3% C alloy.

a given temperature, 650 °C, and a given strain rate, 1.64×10^{-4} s^{-1}. On the same plot, tensile-elongation data of the ingot-processed alloys with carbon contents of less than 2.1% C are also shown. It should be pointed out that all the alloys in the plot have fine grains and a common linear intercept size of about 2 μm. The difference in tensile ductility between the ingot-processed and powder-processed alloys is remarkable. Note that the powder-processed 3% C alloys exhibit tensile elongations almost equivalent to those of the ingot-processed alloys with 1.8% C, whereas a significant difference in tensile ductility is observed between the ingot-processed 3% C alloys and 1.8% C alloys.

The similarity in tensile ductility observed between the two alloys is related to the degree of resistance

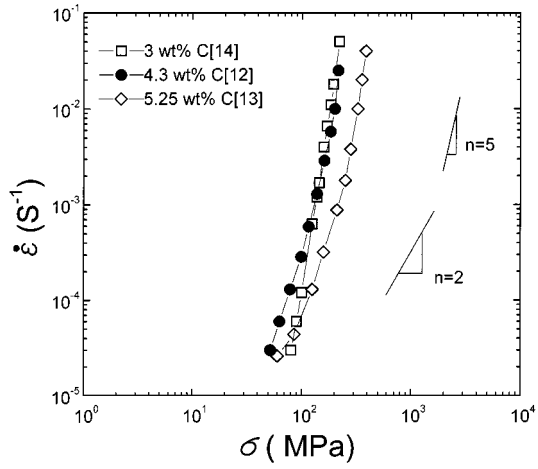

Figure 9 Strain rate-flow stress relationships for the ingot-processed Fe–C alloys.

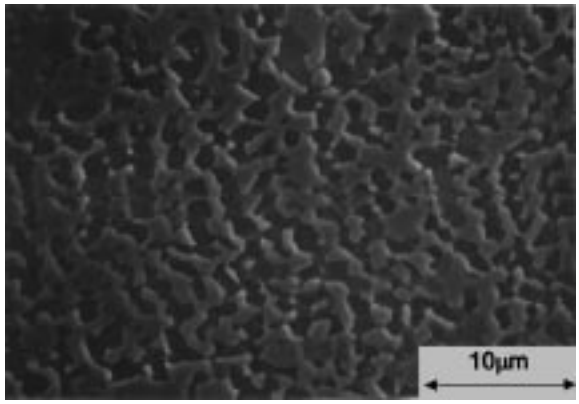

Figure 10 An SEM micrograph of the powder-processed 3% C alloy.

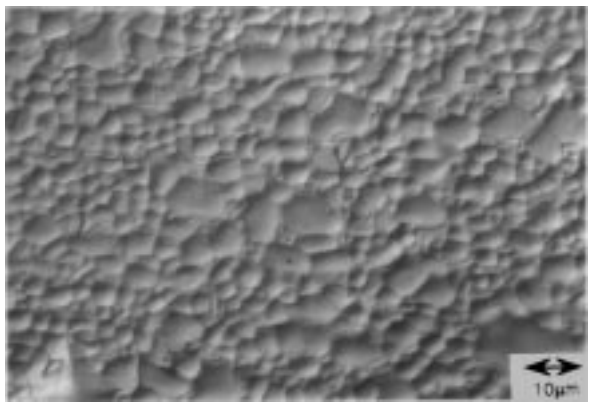

Figure 11 An SEM micrograph of the powder-processed 5.25% C alloy.

against internal cavitation rather than to neck-stability conditions, since both alloys have a similar m value (~ 0.5) at the given testing conditions. This conclusion indicates that ferrite/cementite and ferrite/ferrite interfaces, which are the most abundant types of grain boundaries for 3% C and 1.8% C alloys, respectively, have a similar degree of resistance to cavitation. This result is expected based on the general observation that a similar strength between the two phases minimizes cavitation during superplastic flow. The tensile elongation, however, starts to decrease when cementite becomes the matrix phase. Unlike the ingot-processed alloys, where the decrease of tensile elongation is due to both the presence of coarse cementite and an increase in cementite/cementite boundaries, the decrease of tensile elongation in the powder-processed alloys is primarily due to the latter. Because cementite/cementite grain boundaries have a high grain boundary energy typical of ceramic oxides, they are prone to separation, and low-tensile ductility is the result. In this alloy, multiple-microcracks were frequently observed along cementite/cementite grain boundaries located perpendicular to the tensile axis [10], resulting in a brittle type of fracture (cracking). This type of damage development is often observed in the fine-grained ceramic oxides deforming superplastically. Unlike in the 5.25% C alloy, however, spherical or elongated cavities are typically observed in alloys with a ferrite matrix, indicating that a ductile failure mechanism occurs like in ordinary superplastic metallic alloys. Fig. 13 is a schematic illustration of cavitation behavior with increasing volume fraction of cementite. As the volume fraction of cementite increases, the cementite phase becomes continuous, and cracks grow along the cementite/cementite grain boundaries, leading to premature failure.

2.3. Tensile elongation as a function of Zener-Hollomon parameter

It was demonstrated by Kim et al. [10] that tensile elongation of superplastic ceramics is dictated by the Zener-Hollomon parameter, $\dot{\varepsilon}\exp(Q_c/RT)$. As the parameter decreases (strain rate decreases or temperature increases), tensile ductility of superplastic ceramics increases. On the other hand, tensile elongations of superplastic metallic alloys is principally determined by neck-stability condition, as controlled by m, rather than the Zener-Hollomon parameter. Fig. 14 compares the tensile elongations of superplastic Fe–C alloys as a function of the Zener-Hollomon parameter. All the tests were performed at temperatures and strain rates which give high m values of ~ 0.5. Two groups of tensile elongation data are available for the 1.3$\sim$1.9% C alloys. One is from material with high amounts of sulfur (low grade) and the other is from material with relatively little sulfur (high grade). The latter exhibits larger tensile elongations than the former. As shown in Fig. 14, although the tensile elongations obtained from the high-and low-grade materials differ, both have similar creep strengths and the same rate-controlling deformation mechanism. Alloys which have a ferrite matrix show no correlation of tensile elongation with $\dot{\varepsilon}\exp(Q_c/RT)$. This is in agreement with the statement that the strain-rate-sensitivity exponent is the principal factor influencing the tensile ductility of superplastic metallic alloys, because it dictates neck formation. On the other hand, the fine-grained 5.25% C material behaves like typical superplastic ceramics. It exhibits a strong correlation of tensile elongation with $\dot{\varepsilon}\exp(Q_c/RT)$ through a wide range of temperatures (725 to 1050 °C) and strain rates (10^{-4} – 10^{-2} s^{-1}). It also shows an increase in tensile ductility with a decrease in $\dot{\varepsilon}\exp(Q_c/RT)$, even though m remains high. This behavior of the 5.25% C alloy can be

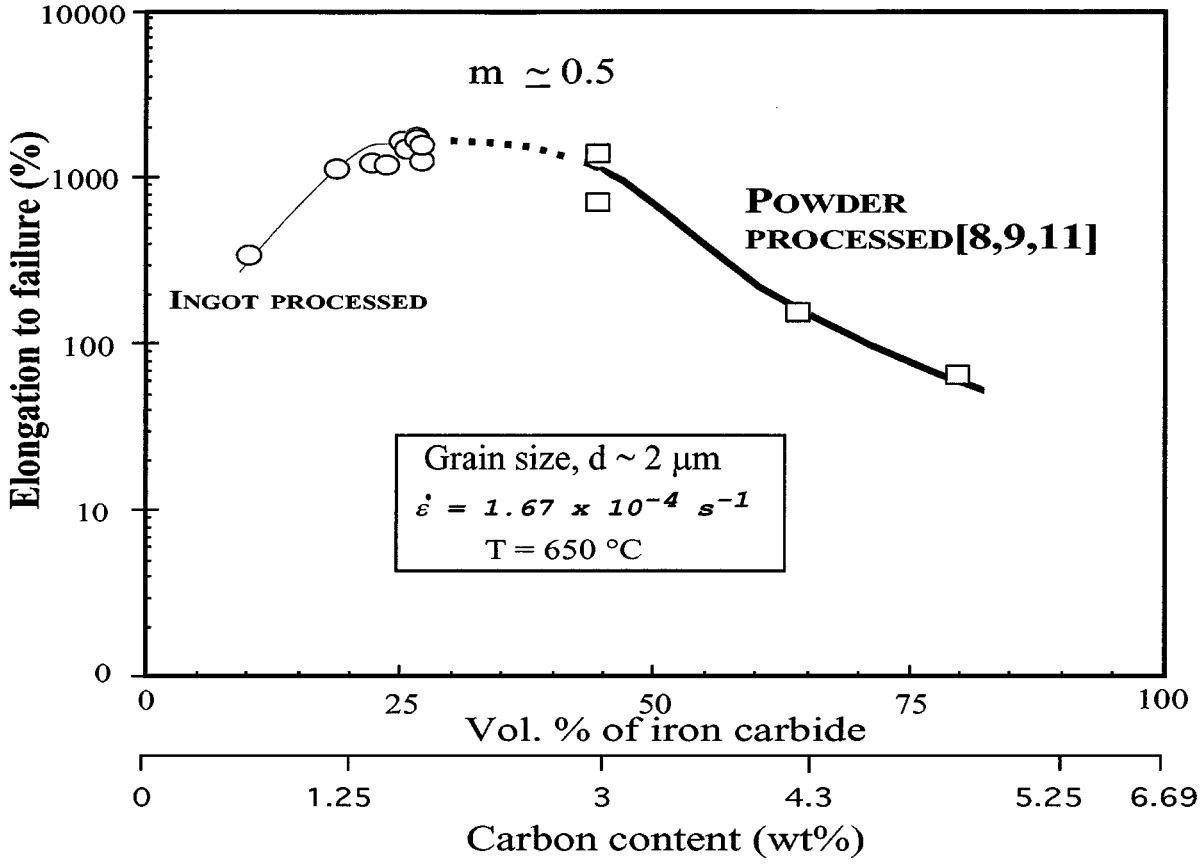

Figure 12 Tensile elongation of powder-processed Fe–C alloys as a function of volume fraction of cementite.

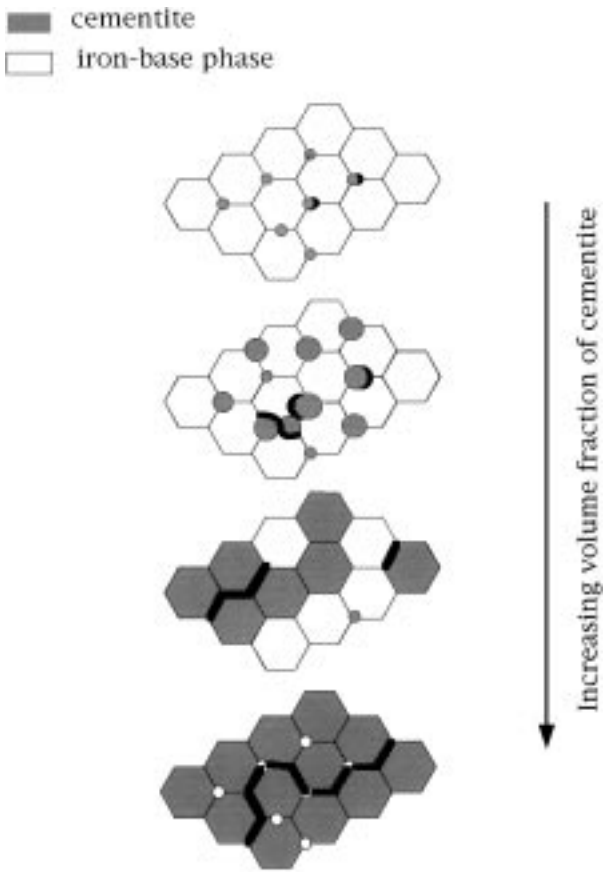

Figure 13 A schematic illustration of cavitation behavior in Fe–C alloys.

attributed to the mechanism by which fine-grained iron-carbide alloys fail. Because cementite/cementite grain boundaries are likely to be separated, as with ceramic oxides, cracks are easily nucleated at these boundaries and propagate normally to the applied tensile stress. A detailed discussion of this is given elsewhere [10]. Only limited data for tensile-elongation behavior of the 4.3% C alloy is available. It is predicted, however, that its behavior is between that of the superplastic metallic alloys and that of superplastic ceramics.

2.4. Temperature range for superplasticity

The temperature range in which the tensile elongations of 400% or larger could be obtained from the fine-grained Fe–C alloys at a strain rate, 1.64×10^{-4} s^{-1} is illustrated by the shaded area on the Fe–C phase diagram in Fig. 15. Such high tensile elongations could be obtained just above or below the A_1 temperature for alloys with 1.8 to 3% C, while a temperature above 1000 °C is required for the 5.25% C alloys. This behavior can be explained as follows. For the low-carbon alloys, the A_1 temperature is the maximum temperature at which a large volume fraction of the second phase (cementite) can be retained. When temperature rises above the A_1 temperature, the volume fraction of cementite decreases and the grain growth rate increases as the result, causing lowered tensile ductility. For the 5.25% alloys, the volume fraction of the second phase

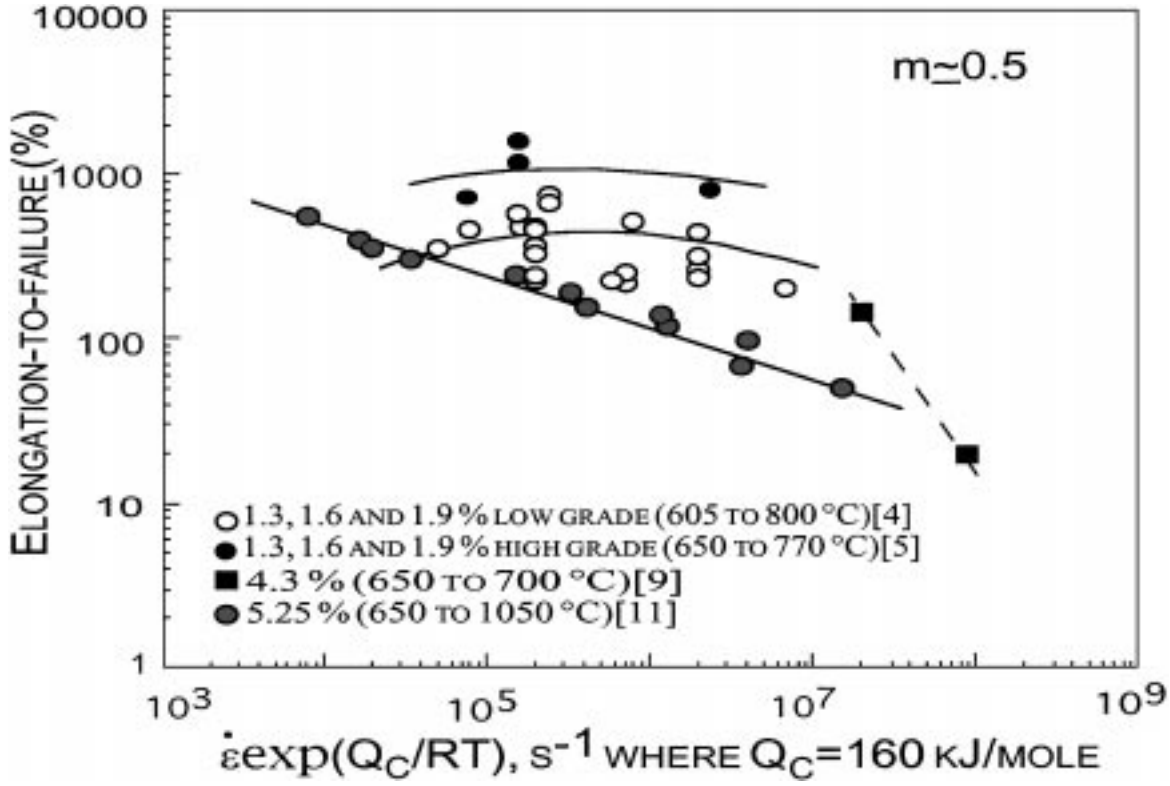

Figure 14 Tensile elongation of Fe–C alloys as a function of Zener-Hollomon parameter.

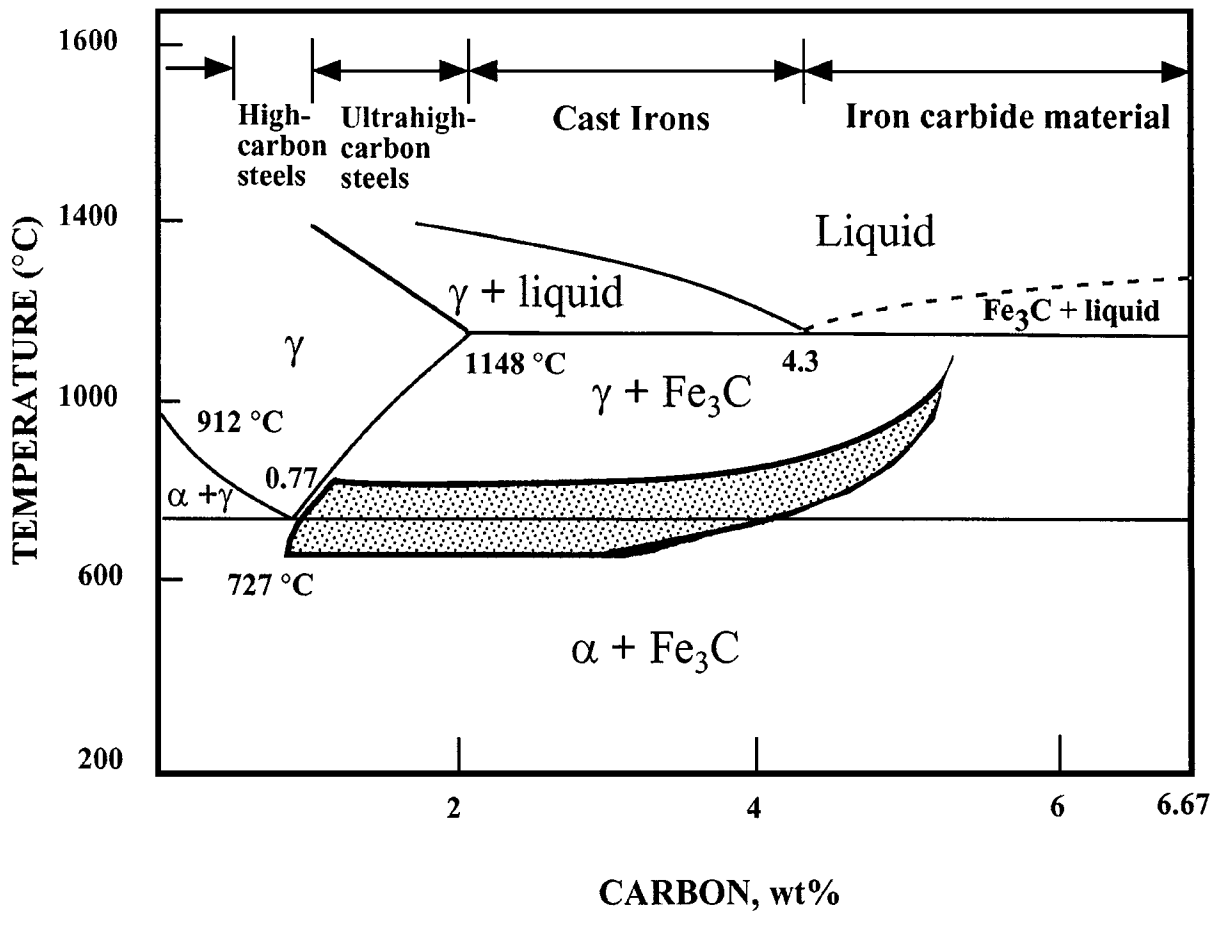

Figure 15 Fe–C phase diagram showing the region where tensile elongations over 400% can be observed at a strain rate of 1.64×10^{-4} s^{-1}.

(ferrite, in this case) increases with temperature. For this reason, the temperature range for superplasticity is moved to higher temperatures. Because cementite/cementite boundaries are easily separated, lower stresses, and lower strain rates or higher temperatures, as given by Equation 1, are required to avoid early failure during tensile deformation. For example, a temperature of 1000 °C is required to sufficiently reduce the flow stress of the 5.25% C alloy in order to obtain tensile elongations of over 400% before failure.

3. Conclusions

1. Stress–strain rate data for Fe–C alloys with a similar grain size (2 μm) and carbon compositions from 1.3 to 5.25% show similar creep strengths.

2. Tensile ductility of ingot-processed Fe–C alloys initially increases with carbon content (volume fraction of cementite) upto 2.1% C. This is because the number of fine cementite particles, available to pin grain boundaries increases as carbon content increases, stabilizing the fine microstructures necessary for superplastic flow. Above 2.1% C, however, the number of coarse cementite particles and the cementite/cementite grain-boundary area increases, and tensile ductility is diminished as the result.

3. Tensile elongation of the powder-processed alloys is considerably larger than that of the ingot-processed alloys for materials with more than 2.1% C.

4. The tensile-elongation behavior of cementite-based alloys is quite different from that of iron-based alloys when compared as a function of the Zener-Hollomon parameter.

5. The optimum temperature range for achieving tensile elongations over 400% depends on the volume fraction of cementite.

Acknowledgement

This work has been supported by 97KOSEF.

References

1. J. WADSWORTH, J. H. LIN and O. D. SHERBY, *Met. Techonol.*, 8 (1981) 190.
2. O. D. SHERBY, Tetsu-to-Hagane, **66** (1980) 232.
3. D. W. KIM, T. OYAMA, O. D. SHERBY, O. A. RUANO and J. WADSWORTH, in "Superplastic Forming," ed. S. P. AGRAWAL, (Metals Park, Ohio: The American Society for Metals, 1984) p. 32.
4. B. WALSER and O. D. SHERBY, Metall. Trans. *A*, **10** (1975) 1461.
5. T. OYAMA, J. WADSWORTH, M. KORCHYNSKY and O. D. SHERBY, in the 5th International Conference on the Strength of Metals and Alloys (Aachen, West Germany, 1979) p. 381.
6. O. D. SHERBY et al., in a summary report on Ultrahigh carbon steels, Depart. of Materials Science and Engineering, Stanford University, (1977∼1980) p. 153.
7. J. WADSWORTH and O. D. SHERBY, *Foundary M&T*, (Oct. 1978) 59.
8. O. A. RUANO, L. E. EISELSTEIN and O. D. SHERBY, *Metall. Trans.* A, **13** (1982) 1795.
9. D. W. KUM, G. FROMMEYER, N. G. GRANT and O. D. SHERBY, *Metall. Trans.*, **18A** (1987) 1703.
10. W. J. KIM, J. WOLFENSTINE and O. D. SHERBY, *Acta metall. mater.*, **39** (1991) 199.
11. W. J. KIM, J. WOLFENSTINE, O. A. RUANO, G. FROMMEYER and O. D. SHERBY, *Metall. Trans.*, **23A** (1992) 527.
12. W. J. KIM, O. D. SHERBY, T. G. NIEH and G. FROMMEYER, Scripta Materialia, **35** (1996) 299.
13. W. J. KIM, J. WOLFENSTINE and O. D. SHERBY, *J. of Ceramic Society of Japan*, **102** (1994) 835.
14. W. J. KIM and O. D. SHERBY, Proceedings of the 2nd Pacific Rim International Conference on Advanced Materials and Processing, edited by K. S. Shin, J. K. Yoon and S. J. Kim (The Korean Institute of Metals and Materials, 1995) p. 329.
15. L. HONG, C. F. BURDETT and W. YOUMING, *J. of Material Science*, **28** (1993) 5901.